



Journal Name

ARTICLE

Received 00th January 20xx,

Copper(II)-directed synthesis of neutral heteroditopic [2]rotaxane ion-pair host systems incorporating hydrogen and halogen bonding anion binding cavities

Accepted 00th January 20xx

DOI: 10.1039/x0xx00000x

www.rsc.org/

Asha Brown,^a Katrina M. Mennie,^a Owen Mason,^a Nicholas G. White^b and Paul. D. Beer^{a*}

Neutral heteroditopic [2]rotaxane ion-pair host systems were synthesised via a Cu(II) directed passive metal template strategy. Each rotaxane contains discrete, axle-separated interlocked binding sites for a guest anion and a transition metal counteranion. The anion binding sites are composed of convergent X—H (X = C, N) hydrogen bond donor groups, or mixed X—H and C—I hydrogen and halogen bond donor groups, whereas an equivalent three-dimensional array of amine, pyridine and carbonyl oxygen donor groups comprise the transition metal binding site. ¹H NMR titration experiments in CDCl₃/CD₃OD or CDCl₃/CD₃OD/D₂O solvent mixtures reveal that the heteroditopic [2]rotaxane host systems are capable of cooperative anion recognition in the presence of a co-bound Zn(II) cation.

Introduction

The development of selective receptors and sensors for anions is an important research goal owing to the fundamental roles played by negatively charged species in a range of chemical, medical and environmental processes.^{1–3} One promising approach to the design of selective anion complexants entails the use of mechanically interlocked rotaxane architectures: these molecules can be designed to incorporate shielded, hydrophobic binding cavities whose size and topology complement the geometry and hydrogen-bonding requirements of a target guest anion. We have developed this approach by using the interior cavities of rotaxane molecules as three-dimensional scaffolds on which to append both hydrogen and halogen bond donor groups, enabling the selective recognition of a range of complementary guest anions in competitive solvent media.⁴ By taking advantage of allosteric effects, heteroditopic ion-pair receptors, which contain specific binding sites for both an anion and a counteranion, can offer significantly enhanced anion binding affinities compared to simpler monotopic receptors.^{5,6} However, despite the plentiful examples of non-interlocked ion-pair receptors, reports of interlocked rotaxane-based anion host systems which are capable of simultaneously binding a metal cation are comparatively scarce. Rare examples include heteroditopic rotaxane systems which bind

an anion and an alkali metal, lanthanide or transition metal cation as a contact ion-pair.^{7–10} In addition we have reported a heteroditopic [2]rotaxane host system which recognises halide anions and alkali metal cations in an 'axle-separated' binding fashion,¹¹ along with a number of anion-binding rotaxane and catenanes which incorporate a host-separated transition metal cation as a luminescent or electrochemical reporter group.^{12–18}

Herein we describe the design and synthesis of new neutral heteroditopic [2]rotaxane ion-pair host systems which contain discrete interlocked binding cavities for both an anion and a transition metal cation. The anion and cation recognition sites are separated by the rotaxane's axle component. Convergent hydrogen and halogen bond donor groups are used for anion recognition while the transition metal binding sites are lined with amine, pyridine and carbonyl oxygen groups. The rotaxanes were assembled via a recently developed copper(II) passive template strategy.¹⁹ ¹H NMR titration experiments were used to investigate the anion-recognition properties of the new [2]rotaxane host systems in the presence of a co-bound Zn(II) cation.

Results and discussion

Design and synthesis

The general design of the target heteroditopic [2]rotaxane host systems incorporating individual, axle-separated interlocked binding cavities for an anion and a transition metal counteranion is illustrated schematically in Figure 1.

The macrocycle component integrates an isophthalamide anion recognition site which is located opposite to a tris-amine binding site for transition metal cations. The axle components are also able to simultaneously interact with both an anion and a counteranion, via divergent anion- and cation-binding functional groups. In the first [2]rotaxane design (Figure 1a)

^a Chemistry research laboratory, Department of Chemistry, University of Oxford, Mansfield Road, Oxford, OX1 3TA. E-mail: paul.beer@chem.ox.ac.uk ^b Research School of Chemistry, The Australian National University, Canberra, ACT, Australia. Electronic Supplementary Information (ESI) available: Synthetic procedures and characterisation data; ¹H NMR and UV-visible spectroscopic titration protocols and binding data; crystallographic CIF files and refinement details; selected bond lengths and angles from the X-ray crystal structures. See DOI: 10.1039/x0xx00000x

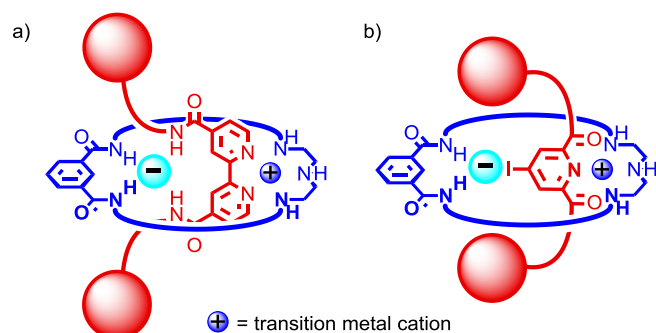
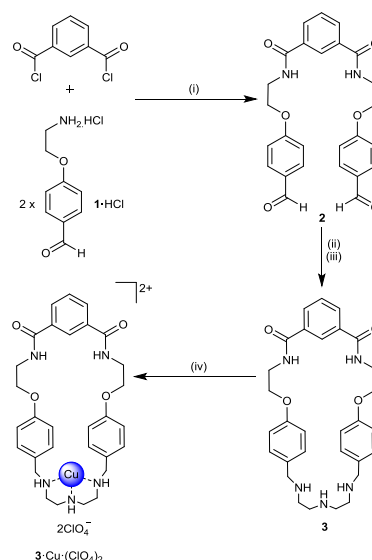


Figure 1. Schematic illustration of the heteroditopic [2]rotaxane ion-pair host systems.

this is achieved using a 2,2-bipyridyl-4,4-bis-amide-functionalised axle component: the bipyridyl nitrogen donor atoms constitute a transition metal chelate ligand, while the amide groups serve as a bidentate hydrogen-bond (HB) donating anion recognition motif. The second [2]rotaxane design (Figure 1b) incorporates an alternative 4-iodopyridyl-2,6-dicarbonyl pyridine-based axle component. It was anticipated that the 2,6-dicarbonylpyridyl functionality would be capable of tridentate complexation to a transition metal cation, while the polarised iodine atom provides a potential halogen-bond (XB) donating anion binding locus. Halopyridin(ium) motifs have not yet been widely explored as a class of XB donor in the anion coordination field,^{20–22} where the majority of studies have so far focused on haloimidazolium, halotriazole/triazolium and haloperfluoroarene XB donor groups.²³

Synthesis of macrocycle component. The macrocycle component of the rotaxanes was prepared by adaptation of the one-pot, two step reductive amination reaction employed by Ghosh and co-workers for the synthesis of related tris-amine-functionalised cyclic structures.^{19,24,25} Condensation of isophthaloyl dichloride with two equivalents of the primary amine-derivative **1**·HCl provided the requisite bis-aldehyde precursor **2** in 44% yield. Sequential treatment of the bis-aldehyde with bis(2-aminoethyl)amine followed by NaBH₄ in CH₂Cl₂/MeOH afforded macrocycle **3** in 70% yield. After stirring macrocycle **3** with Cu(ClO₄)₂·6H₂O in CH₂Cl₂:MeOH 1:1, the corresponding copper(II) complex **3**·Cu(ClO₄)₂ was isolated in 98% yield (Scheme 1).

Crystals of macrocycle **3**·Cu(ClO₄)₂ suitable for X-ray structural determination were grown by layered diffusion of di-isopropyl ether into a CH₃CN solution of the complex. In the solid state the Cu(II) centre is coordinated to the macrocycle's three secondary amine nitrogen donor atoms N20, N23 and



Scheme 1. Synthesis of the Cu(II)-complexed tris-amine/isophthalamide-functionalised macrocycle **3**·Cu(ClO₄)₂. *Reagents and conditions:* (i) 4-dimethylaminopyridine, Et₃N, CH₂Cl₂, r.t., 48 h, 44%; (ii) diethylenetriamine, CH₂Cl₂, MeOH, r.t., overnight; (iv) NaBH₄, CH₂Cl₂, MeOH, r.t., 6 h, 70%; (v) Cu(ClO₄)₂·6H₂O, CH₂Cl₂, MeOH, r.t., 18 h, 98%.

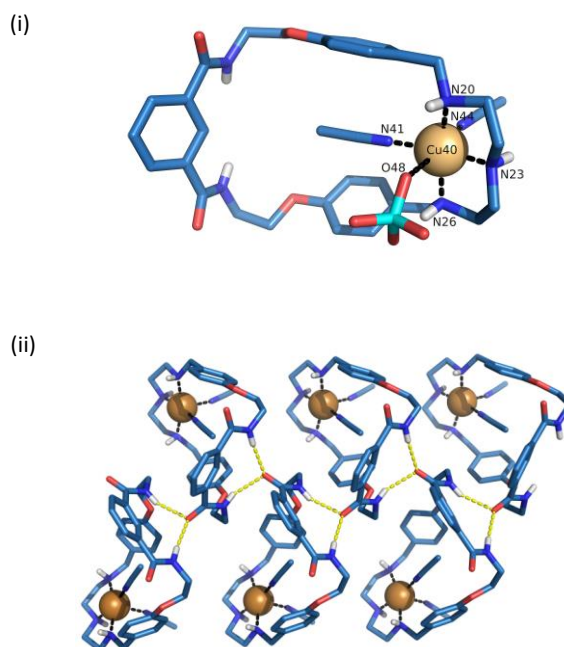
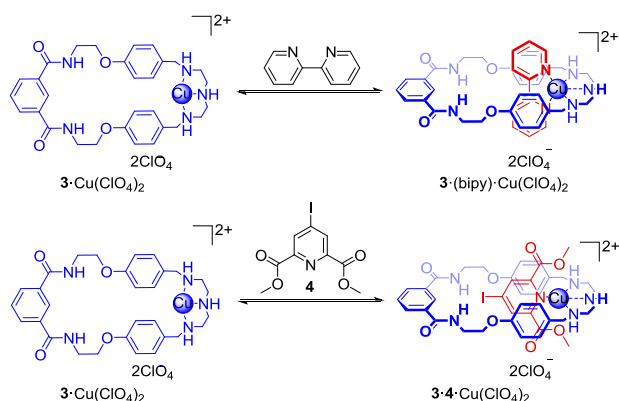


Figure 2. Solid state structure of the macrocyclic Cu(II) complex **3**·Cu(ClO₄)₂: (i) content of the asymmetric unit; (ii) infinite zig-zag chain formed through intramolecular NH...O hydrogen bonding interactions. Non-polar hydrogen atoms, non-coordinating solvent molecules and the non-coordinating perchlorate counteranion have been omitted for clarity.

N26 (Cu40—N distances: 2.086[4], 2.071[3] and 1.994[4] Å) in addition to two acetonitrile solvate molecules (Cu40—N41 and Cu40—N44 distances: 2.009[4] and 2.190[5] Å) in an almost perfect ($\tau = 0.035$)²⁶ square pyramidal coordination geometry. A weakly coordinating perchlorate anion is also located in proximity to the Cu(II) cation (Cu40—O48 distance: 2.829[4] Å). The isophthalamide group is held in a *syn-syn* conformation by NH...O hydrogen bonding interactions with a carbonyl group of an adjacent macrocycle; these intermolecular hydrogen bonding interactions link the macrocycle molecules in an infinite zig-zag chain which is aligned with the crystallographic *a* axis (Figure 2).[¶]

Pseudorotaxane assembly investigations. Recently Ghosh and co-workers have demonstrated copper(II)-templated pseudorotaxane assembly between a tris-amine-functionalised macrocycle and a range of bipyridine, phenanthroline and 2-pyridyl-benzimidazole threading compounds.^{19,24,25,27–29} Similarly, evidence for the formation of copper(II)-templated pseudorotaxane assemblies between the new isophthalamide-containing copper-complexed macrocycle **3**·Cu(ClO₄)₂ and 2,2-bipyridyl and 4-iodopyridyl-2,6-dicarbonyl threading ligands was obtained using UV-visible spectroscopy and X-ray crystallography techniques. For the purposes of the pseudorotaxane assembly investigations unsubstituted 2,2-bipyridine was used as a model threading ligand in place of a 4,4-bis-amide functionalised analogue owing to the prohibitively low solubilities of simple 4,4-bis-amide functionalised 2,2-bipyridine derivatives (Scheme 2).



Scheme 2. Copper(II)-template formation of pseudorotaxane assemblies comprising macrocycle **3** and 2,2-bipyridine or 4-iodopyridyl threading ligands

Titration of 2,2-bipyridine and 4-iodopyridyl-2,6-dicarbonyl into a 3 mM solution of the macrocycle **3**·Cu(ClO₄)₂ in CH₃CN induced gradual bathochromic shifts in the maximum absorbance of the Cu(II) d–d transitions (Figure 3 and Figure S18, ESI). Global fitting of the titration data using Specfit³⁰ software indicated a 1:1 stoichiometric association constant of $K = 2352$ (19) M^{–1} for the pyridyl-threaded pseudorotaxane assembly **3**·**4**·Cu(ClO₄)₂ in CH₃CN. The equilibrium constant for the assembly of the more stable **3**·2,2-bipyridine·Cu(ClO₄)₂ complex was observed to be too high to allow accurate data fitting at the millimolar concentrations of the titration experiment and a lower limit of $K > 10^4$ M^{–1} was therefore estimated, in both CH₃CN and the more competitive solvent DMSO.

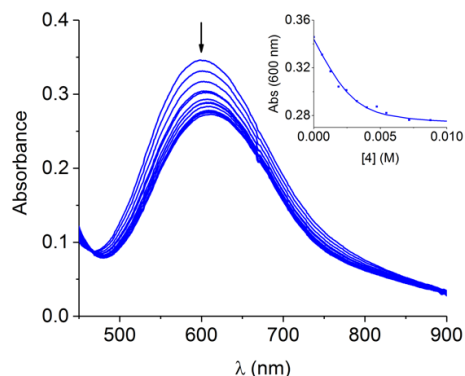


Figure 3. Changes in the visible absorption spectra of a 3 mM solution of macrocycle **3**·Cu(ClO₄)₂ in CH₃CN on addition of an increasing concentration of compound **4**. Inset: change in absorbance at 600 nm as a function of [**4**]. The square data points represent experimental data; the continuous line represents the calculated binding isotherm for $K = 2352$ M^{–1}.

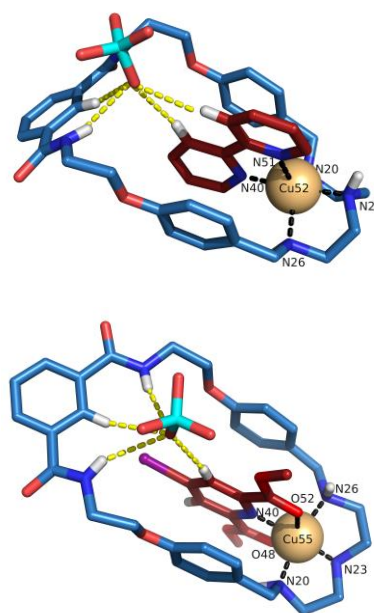


Figure 4. Solid state structures of the pseudorotaxane assemblies **3**·2,2-bipyridine·Cu(ClO₄)₂ (top) and **3**·**4**·Cu(ClO₄)₂ (bottom). For clarity, non-polar hydrogen atoms, non-coordinating solvent molecules and non-coordinating perchlorate counteranions have been omitted, and only one of the two crystallographically independent pseudorotaxane complexes contained within the asymmetric unit is shown for the **3**·2,2-bipyridine·Cu(ClO₄)₂ structure.

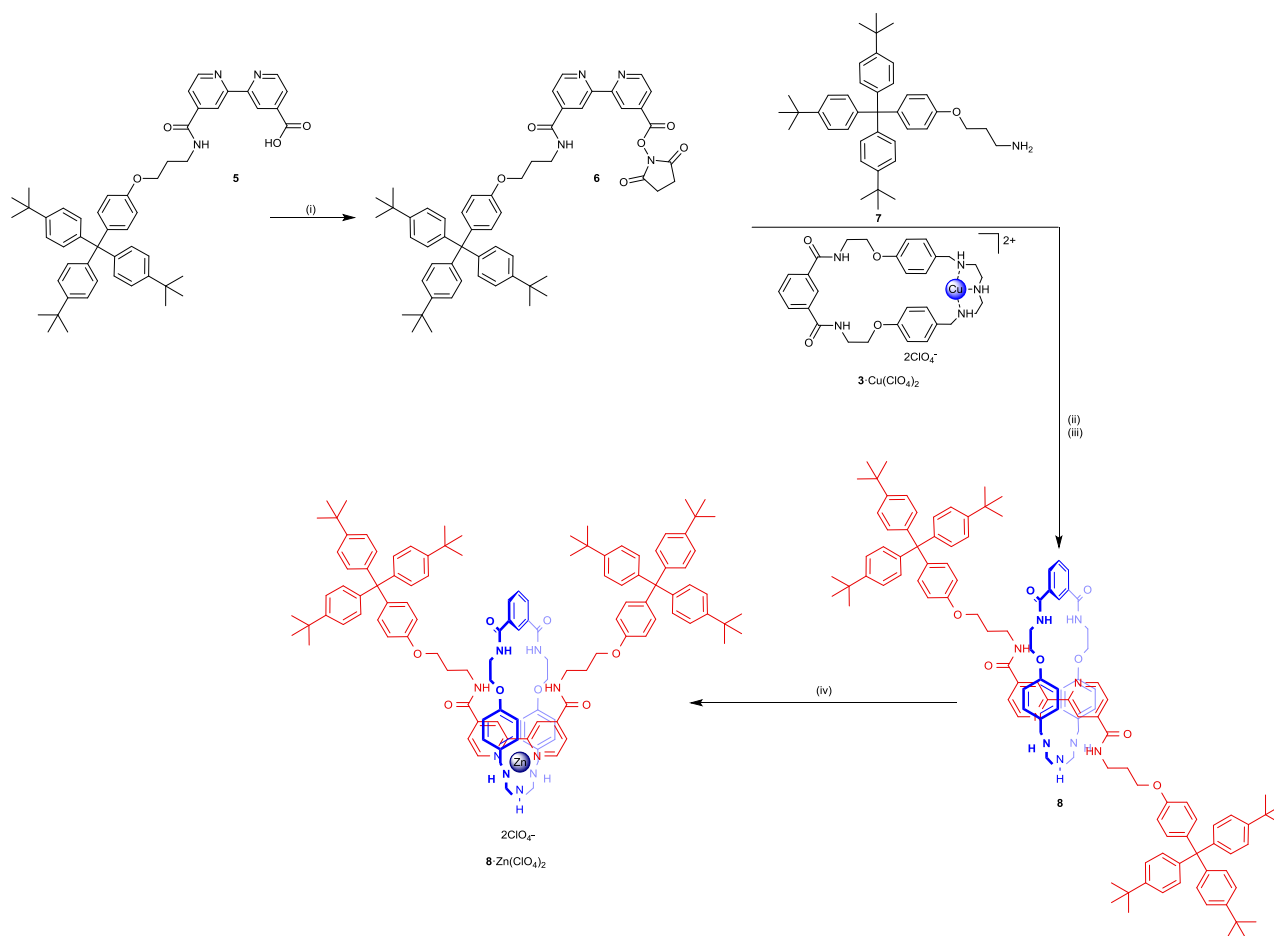
The pseudorotaxane assemblies were also characterised in the solid state (Figure 4). Crystals suitable for X-ray structural determination were grown by layered diffusion of diisopropyl ether into a CH₃CN solution of macrocycle **3**·Cu(ClO₄)₂ containing an excess of 2,2'-bipyridine or the iodopyridyl compound **4**. For the **3**·2,2-bipyridine·Cu(ClO₄)₂ structure the asymmetric unit contains two crystallographically independent pseudorotaxane complexes. In each of the independent complexes the copper (II) centre is coordinated to the two nitrogen atoms of the 2,2'-bipyridyl moiety (Cu—N distances: 2.002[4]–2.078[4] Å) and three nitrogen atoms of the

macrocycle diethylenetriamine group (Cu—N distances: 2.019[4]–2.198[4] Å) in a distorted trigonal bipyramidal arrangement ($\tau = 0.80, 0.68$),²⁶ and a parallel stacking arrangement between the macrocycle aromatic 4-alkoxybenzyl and interpenetrated 2,2'-bipyridyl groups is observed. In addition, a perchlorate counteranion is held in close proximity to each of the macrocycle's isophthalamide binding cleft by short NH—O and CH—O contacts.

In the solid state structure of the **3·4**·Cu(ClO₄)₂ assembly the 2,6-pyridyl-bis-ester threading component similarly interpenetrates the macrocycle's cavity, with the iodine XB donor substituent projecting towards the macrocycle's isophthalamide binding cleft. Coordinative bonds between the Cu(II) cation and the pyridyl nitrogen and carbonyl oxygen atoms of the 4-iodopyridyl-2,6-bis-ester moiety are observed (Cu55—N40 distance: 2.030[5] Å; Cu55—O48 and Cu55—O52 distances: 2.370[5] and 2.406[55] Å). Three additional Cu—N bonds between the Cu(II) cation and the macrocycle secondary amine nitrogen atoms N20, N23 and N26 (Cu55—N distances: 1.909[17]–2.090[5] Å) complete the cation's distorted octahedral coordination sphere. A perchlorate counteranion is again held in close proximity to the macrocycle's isophthalamide binding cleft by a series of C—H·····O and N—H·····O hydrogen-bonding interactions.¶

Synthesis and Characterisation of [2]Rotaxanes

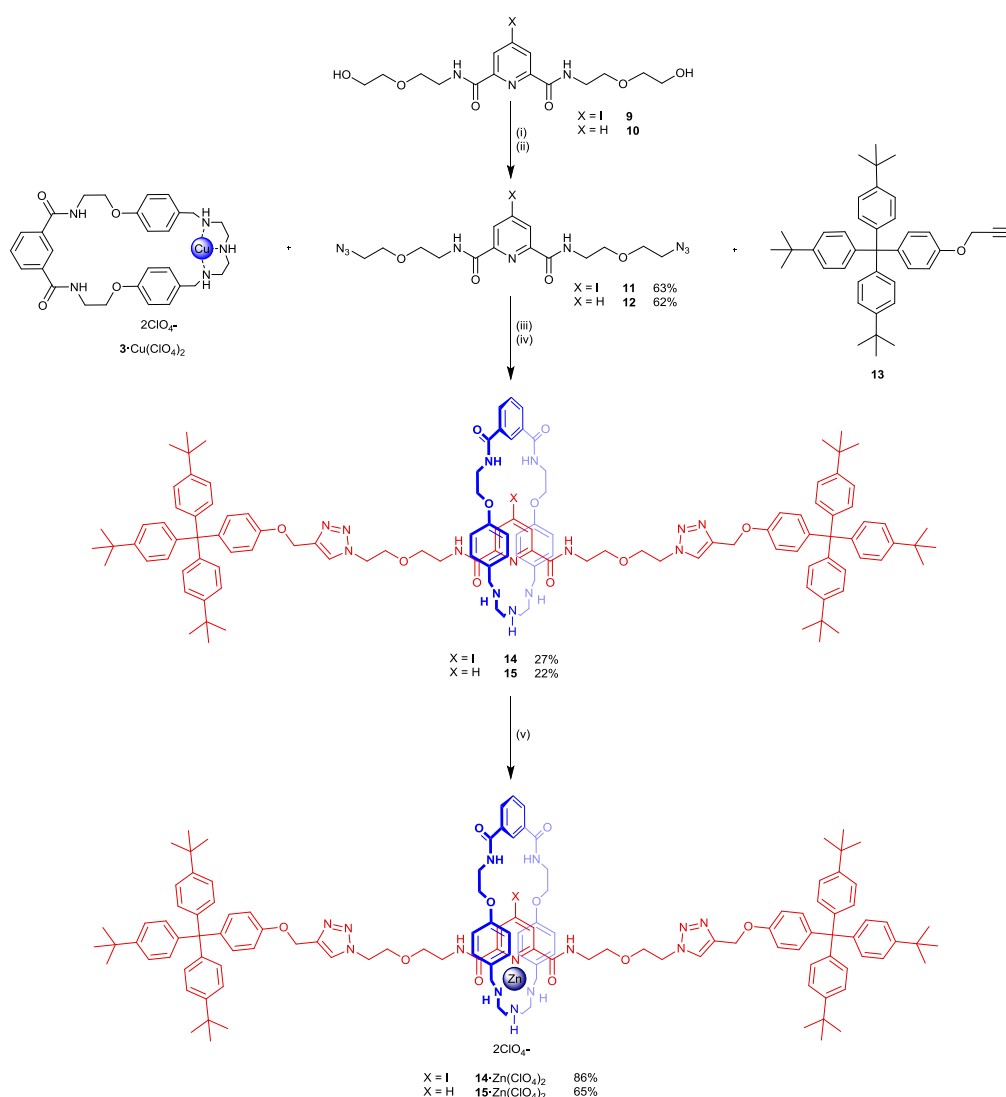
Synthesis of a [2]rotaxane incorporating a hydrogen bonding 2,2-bipyridyl bis-amide axle component. The target 2,2-bipyridyl 4,4-bis-amide containing [2]rotaxane **8** was prepared via a mono-stoppering strategy, as illustrated in Scheme 3. An amide coupling reaction was employed during the key rotaxane-forming step. Reaction of the carboxylic acid derivative **5** (prepared by a multi-step procedure described in the supporting information) with *N*-hydroxysuccinimide in the presence of dicyclohexylcarbodiimide (DCC) yielded the activated ester **6**, which was immediately reacted with the primary amine-functionalised stoppering compound **7**³¹ in the presence of the macrocycle **3**·Cu(ClO₄)₂ in CH₃CN/CH₂Cl₂ 1/1. In order to facilitate purification and characterisation of the [2]rotaxane product, the paramagnetic Cu(II) cation template was removed by extraction with an aqueous EDTA/NH₄OH solution during work-up. Subsequent purification by preparative thin layer chromatography (CH₂Cl₂/MeOH/sat. NH₄OH_(aq)) afforded the metal-free rotaxane **8** in 24% yield. In preparation for ¹H NMR titration experiments, rotaxane **8** was then stirred with Zn(ClO₄)₂ in CH₂Cl₂/MeOH to provide the diamagnetic zinc-complexed rotaxane **8·Zn(ClO₄)₂** in 82% yield after recrystallisation.



Scheme 3. Synthesis of the [2]rotaxane **8·Zn(ClO₄)₂**. Reagents and conditions: (i) *N*-hydroxysuccinimide, *N,N'*-dicyclohexylcarbodiimide, CH₂Cl₂, r.t., 18 h; (ii) Et₃N, CH₂Cl₂, CH₃CN, r.t., 72 h; (iii) EDTA/NH₄OH(aq), 24%; (iv) Zn(ClO₄)₂·6H₂O CH₂Cl₂, MeOH, r.t., 1 h. 82%.

Synthesis of a [2]rotaxane incorporating a halogen bonding 4-iodopyridyl-2,6-dicarbonyl axle component Initial attempts to employ an analogous activated ester stoppering strategy to the synthesis of a halogen bonding rotaxane incorporating a 4-iodopyridyl-2,6-bisester axle centrepiece proved to be very low yielding and inefficient. In addition, during the course of these preliminary experiments we observed the 2-iodopyridyl-2,6-bis-ester motif to be unstable towards ester hydrolysis and

subsequent decarboxylation during chromatographic purification on silica. An alternative Cu(I)-catalysed azide-alkyne cycloaddition (CuAAC) based stoppering methodology was therefore used to synthesise a halogen bonding rotaxane incorporating a 4-iodopyridyl axle component, and amide functional groups were installed in place of ester groups at the 2 and 6 positions on the pyridine ring in order to provide greater chemical stability (Scheme 4).



Scheme 4. Synthesis of the [2]rotaxanes **14·Zn(ClO₄)₂** and **15·Zn(ClO₄)₂**. *Reagents and conditions:* (i) methanesulfonyl chloride, Et₃N, CH₂Cl₂, 0 °C to r.t.; (ii) NaN₃, DMF, 50 °C; (iii) Cu(CH₃CN)₄PF₆, TBTA, DiPEA, CH₂Cl₂, CH₃CN, r.t., 48 h; (iv) EDTA/NH₄OH_(aq); (v) Zn(ClO₄)₂·6H₂O, CH₂Cl₂, MeOH, r.t., 1 h.

A solid state structure of the complex **3·9·Cu(ClO₄)₂** provides confirmation of the successful Cu(II) directed formation of an

orthogonal pseudorotaxane assembly between the tris-amine macrocycle and the modified bis-amide based threading ligand

(Figure 5).[¶] The bis-azide-terminated threading compound **11** was therefore stirred with two equivalents of the alkyne-functionalised stoppering compound **13**³² in the presence one equivalent of the macrocycle **3**-Cu(ClO₄)₂, Cu(CH₃CN)₄PF₆, TBTA and DiPEA in a CH₂Cl₂/CH₃CN solvent mixture. After treatment of the crude product with EDTA/NH₄OH_(aq), the metal-free rotaxane **14** was purified by preparative thin layer chromatography and isolated in 27% yield. The Zn(II) complex **14**·Zn(ClO₄)₂ was obtained in 86% yield by treatment of compound **14** with Zn(ClO₄)₂·6H₂O. For comparison purposes the analogous [2]rotaxane **15**·Zn(ClO₄)₂ which lacks the iodine halogen bond donor substituent was also synthesised via the same method and obtained in comparable yield.

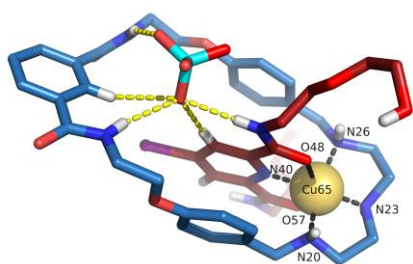


Figure 5. Solid state structure of the pseudorotaxane assembly **3**·**9**·Cu·(ClO₄)₂. For clarity, non-polar hydrogen atoms, non-coordinating solvent molecules and non-coordinating perchlorate counteranions have been omitted.

Characterisation of metal-free [2]rotaxanes. The metal-free rotaxanes **8**, **14** and **15** were fully characterised by electrospray mass spectrometry and ¹H and ¹³C NMR spectroscopies. A comparison of the ¹H NMR spectrum of the metal-free [2]rotaxane **8** with those of its non-interlocked macrocycle and axle components **ϕ** in CDCl₃/CD₃OD (Figure 6(i)) reveals significant upfield shifts in the signals for the aromatic macrocycle aromatic 4-alkoxybenzene protons f and g and bipyridine protons 2 and 3 upon formation of the [2]rotaxane. This is suggestive of mutual shielding of the aromatic π systems by stabilising donor-acceptor interactions. Further evidence for this is provided by the observation of through-space ROE interactions between protons 2 and 3 and f and g in the 2-D ROESY spectrum of the rotaxane (Figure 6(ii)). Similar upfield perturbations in the shifts of the macrocycle protons f and g were observed upon formation of the 4-iodopyridyl containing rotaxane **14** (Figure 7), suggesting the existence of similar intercomponent aromatic donor-acceptor interactions in this [2]rotaxane. However for this system no through-space interactions between the interlocked components were observed by ROESY spectroscopy, possibly as a result of the fluxional dynamic nature of the system.

Characterisation of Zn(II)-complexed [2]rotaxanes Successful formation of the three Zn(II) rotaxane complexes was evidenced by MALDI mass spectrometry, which revealed peaks centred at 1927.2, 2197.8 and 2071.1, corresponding to the [M – 2ClO₄ – H]⁺ ions for compounds **8**·Zn(ClO₄)₂, **14**·Zn(ClO₄)₂

and **15**·Zn(ClO₄)₂ respectively. The ¹H NMR spectrum of the Zn(II) complex **8**·Zn(ClO₄)₂ is compared with that of the metal-free rotaxane **8** in Figure 8. In the presence of the Zn(II) cation the two sides of the axle become inequivalent on the timescale of the NMR experiment as a result of slower dynamic conformational interconversion, and a splitting of the majority of the axle proton signals and macrocycle CH₂ proton signals is consequently observed, consistent with a reduction from C_{2v} point group symmetry to lower Cs symmetry. The aromatic bipyridine protons 1 and 2 and macrocycle ethylene CH₂ protons i and j are deshielded by the presence of the cation within the metal binding cavity. Conversely, the signals for the macrocycle aromatic protons f and g undergo significant upfield shifts, presumably because the Zn(II) cation locks the macrocycle and axle components in a co-conformation in which the π electron clouds of the axle bipyridyl and macrocycle 4-alkoxybenzene groups overlap. ROESY spectroscopy indicated several through-space coupling interactions between the bipyridyl protons 1, 1', 2', 3 and 3' and the macrocycle aromatic protons f and g, as well as one between the internal macrocycle proton c and internal bipyridyl aromatic proton 3', which is consistent with the proposed conformation in which the axle bipyridine group is

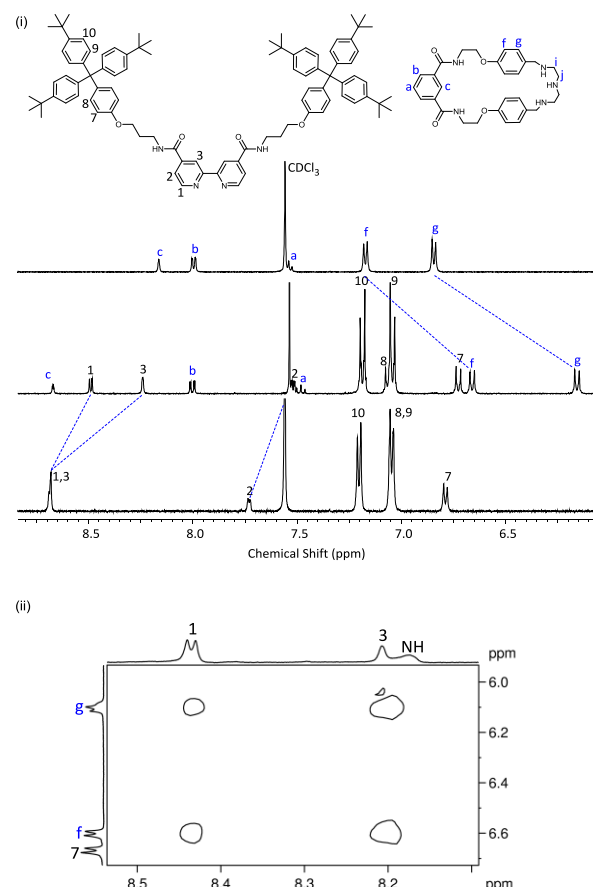


Figure 6. (i) Comparative partial ¹H NMR spectra of the macrocycle tris-amine macrocycle **3** (top), [2]rotaxane **8** (middle) and non-interlocked axle component **ϕ** in 1:1 CDCl₃:CD₃OD at 293 K; (ii) section of the ¹H-¹H ROESY NMR spectrum of the metal-free rotaxane **8** in 1:1 CDCl₃:CD₃OD at 293 K.

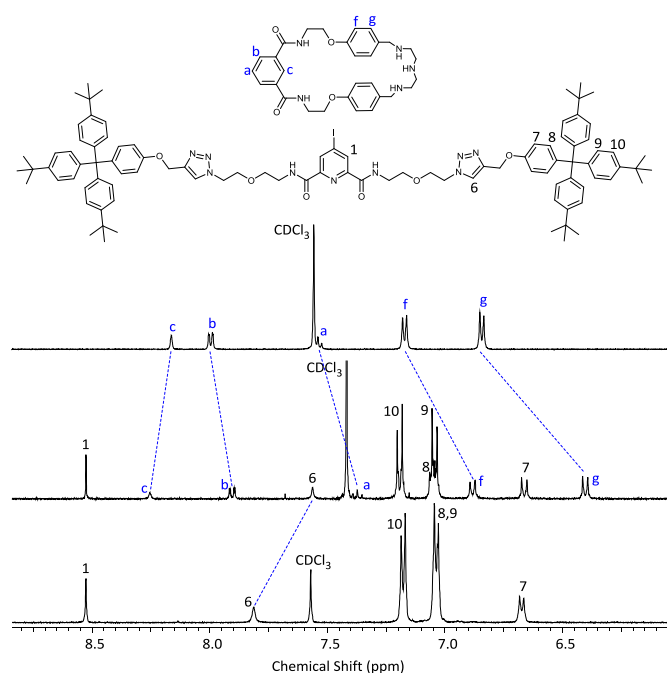


Figure 7. (i) Comparative partial ^1H NMR spectra of the macrocycle tris-amine macrocycle **3** (top), [2]rotaxane **14** (middle) and non-interlocked axle component ϕ in 1:1 CDCl_3 : CD_3OD at 293 K.

intercalated between the macrocycle 4-alkoxybenzene groups, with the isophthalamide and bipyridyl-bis-amide groups converging towards a central anion binding cavity (Figure S8, ESI).

Similar effects were observed upon complexation of $\text{Zn}(\text{II})$ to the pyridyl-containing [2]rotaxanes **14** and **15**. Illustrative spectra for the 4-iodopyridyl-functionised rotaxane **14** and its $\text{Zn}(\text{II})$ complex **14**- $\text{Zn}(\text{ClO}_4)_2$ are shown in Figure 9. The observed splitting of the axle proton signals and diastereotopic splitting of the macrocycle CH_2 proton signals again suggests a reduction from the original C_{2v} symmetry of the metal-free rotaxane **14** upon metal binding. Both the axle iodopyridyl proton signal $1'$ and macrocycle alkoxybenzene signals f and g are observed to shift upfield in the presence of the $\text{Zn}(\text{II})$ cation. In addition through space interactions between protons f and g and 1 and $1'$ are observed in the ROESY spectrum (Figure S16, ESI), consistent with an interlocked co-conformation which involves parallel face-to-face stacking between the 4-alkoxybenzene and 4-iodopyridine functional groups.

Anion recognition properties of the heteroditopic [2]rotaxanes

[2]Rotaxane 8- $\text{Zn}(\text{ClO}_4)_2$. The anion recognition properties of the $\text{Zn}(\text{II})$ -complexed rotaxane **8**- $\text{Zn}(\text{ClO}_4)_2$ were probed by ^1H NMR titration experiments in CDCl_3 : CD_3OD 1:1. The tetrabutylammonium salts of a range of halide and oxoanions were titrated into a solution of the rotaxane in CDCl_3 : CD_3OD 1:1, which resulted in perturbations of the chemical shifts signals of protons 1–3, $1'$ – $3'$ and c which surround the rotaxane's interlocked binding cavity. In all cases the kinetics of exchange were observed to be fast on the ^1H NMR timescale at 500 MHz, allowing association constants to be

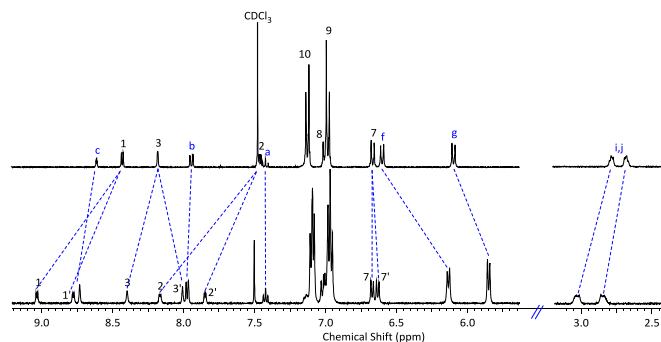


Figure 8. Partial ^1H NMR spectra of the metal free rotaxane **8** (top) and zinc-complexed rotaxane **8**- $\text{Zn}(\text{ClO}_4)_2$ (bottom) in CDCl_3 : CD_3OD 1:1 at 298 K. Proton assignments for compound **8** are shown in Figure 6.

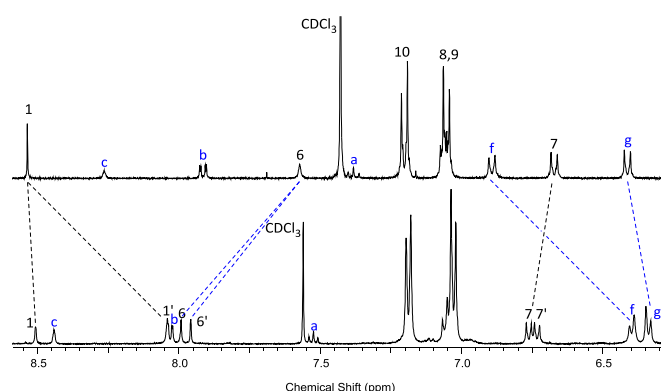


Figure 9. Partial ^1H NMR spectra of the metal free rotaxane **14** (top) and zinc-complexed rotaxane **14**- $\text{Zn}(\text{ClO}_4)_2$ (bottom) in CDCl_3 : CD_3OD 1:1 at 298 K. Proton assignments for compound **14** are shown in Figure 7.

calculated by fitting the chemical shift changes of the internal macrocycle proton c to a 1:1 stoichiometric binding model using WinEQNMR³³ software (Table 1 and Figure S19, ESI). Addition of chloride, bromide, iodide and nitrate anions induced downfield shifts in the signals for the internal axle bipyridine proton 3 and macrocycle isophthalamide proton c , consistent with multidentate hydrogen bond donation from the axle bipyridine and macrocycle isophthalamide groups to the encapsulated guest anion (Figure 10). The calculated association constants (Table 1) reveal a selectivity for Cl^- and Br^- over I^- and NO_3^- which can be attributed to a combination of size-complementary, anion basicity and anion solvation effects. The rotaxane's overall selectivity for acetate anions is incongruent with the selectivity behaviour exhibited by structurally related interlocked host molecules, which have previously been shown to bind chloride and bromide anions in preference to more basic acetate anions owing to the superior size-complementarity between these spherical halide anions and the interlocked binding cavities of the host molecule.^{13,34} A possible explanation is that the [2]rotaxane **8**- $\text{Zn}(\text{ClO}_4)_2$ interacts with acetate anions via a different binding mode involving direct ligation of the acetate anion to the $\text{Zn}(\text{II})$ cation. This is supported by analysis of the chemical shift changes of the bipyridine protons 1 and $1'$, which move upfield in the presence of acetate, but downfield in the presence of halide anions (Figure S20, ESI).

Notably, negligible spectral perturbations were observed when halide anions were added to $\text{CDCl}_3/\text{CD}_3\text{OD}$ solutions of the neutral [2]rotaxane **8** in the absence of a co-bound $\text{Zn}(\text{II})$ cation, which highlights the important role of the metal ion in cooperatively enhancing the rotaxane's anion binding affinities via a combination of preorganisation and electrostatic effects.

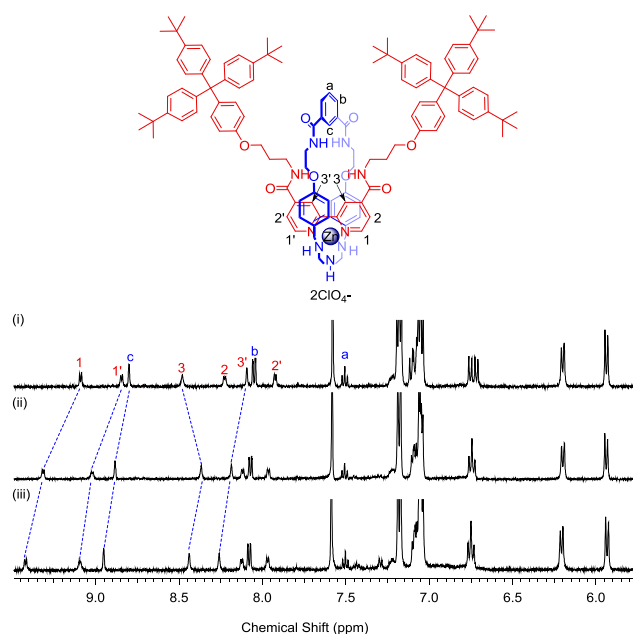


Figure 10. Partial ^1H NMR spectra of the [2]rotaxane **8**- $\text{Zn}(\text{ClO}_4)_2$ in the presence of (i) 0, (ii) 1 and (iii) 5 equivalents of TBACl in $\text{CDCl}_3:\text{CD}_3\text{OD}$ 1:1 at 298 K

Table 1. Stability constants, K (M^{-1}), for 1:1 complexes of the [2]rotaxane host systems **8**- $\text{Zn}(\text{ClO}_4)_2$, **14**- $\text{Zn}(\text{ClO}_4)_2$ and **15**- $\text{Zn}(\text{ClO}_4)_2$ with various anions in $\text{CDCl}_3:\text{CD}_3\text{OD}$ 1:1 or $\text{CDCl}_3:\text{CD}_3\text{OD}:\text{D}_2\text{O}$ 45:45:10 at 298 K

X^-	$K(\text{M}^{-1})^a$		
	8 - $\text{Zn}(\text{ClO}_4)_2^b$	14 - $\text{Zn}(\text{ClO}_4)_2^c$	15 - $\text{Zn}(\text{ClO}_4)_2^c$
Cl^-	1160	535	500
Br^-	920	1080	925
I^-	165	830	540
AcO^-	$> 10^4$	^d	–
NO_3^-	270	570	315

^aDetermined by fitting changes in the chemical shift of the internal macrocycle proton c to a 1:1 stoichiometric binding isotherm using WinEQNMR³³ software. Errors associated with the curve fitting process (estimated expanded uncertainties at the 95% confidence interval level) are $<10\%$. All anion added as TBA salts. ^bIn $\text{CDCl}_3:\text{CD}_3\text{OD}$ 1:1. ^cIn $\text{CDCl}_3:\text{CD}_3\text{OD}:\text{D}_2\text{O}$ 45:45:10. ^dAddition of TBAACO resulted in the appearance of rotaxane a new set of ^1H NMR signals in slow exchange with the spectrum of the original zinc(II) complexed rotaxane, which was attributed to direct acetate anion ligation to the metal cation.

[2]Rotaxane 14-Zn(ClO₄)₂. For the [2]rotaxane **14**- $\text{Zn}(\text{ClO}_4)_2$, ^1H NMR titration experiments were performed in a more competitive aqueous-organic solvent mixture $\text{CDCl}_3:\text{CD}_3\text{OD}:\text{D}_2\text{O}$ 45:45:10. Addition of the TBA salts of halide and nitrate anions to a 1.5 mM solution of the host in this solvent mixture induced progressive downfield shifts in the aromatic cavity proton signals 2' and c (Figure 11). In contrast, on addition of TBAOAc a new set of peaks appeared in slow exchange with the original signals, which may again

indicate a different binding mode involving direct ligation of the acetate anion to the metal cation. Stoichiometric 1:1 association constants for the halide and nitrate anions were determined by WinEQNMR³³ analysis of the titration data, monitoring proton c (Table 1 and Figure S21, ESI). The association constants displayed in Table 1 for both the iodo-pyridine-functionalised XB rotaxane. **14**- $\text{Zn}(\text{ClO}_4)_2$ and C—H hydrogen bonding analogue **15**- $\text{Zn}(\text{ClO}_4)_2$ show in general that both rotaxanes exhibit less effective discrimination between the halide and nitrate anions compared to the bipyridyl rotaxane system **8**- $\text{Zn}(\text{ClO}_4)_2$. For rotaxanes **14**- $\text{Zn}(\text{ClO}_4)_2$ and **15**- $\text{Zn}(\text{ClO}_4)_2$ the binding affinities for bromide, iodide and nitrate with respect to chloride are increased, and an overall preference for bromide is observed. This trend may be partially influenced by solvation factors: it is likely that the addition of a 10% volume of D_2O to the solvent mixture would result in a larger increase in the competitive desolvation penalty for the relatively hydrophilic chloride anion than for the more hydrophobic bromide, iodide and

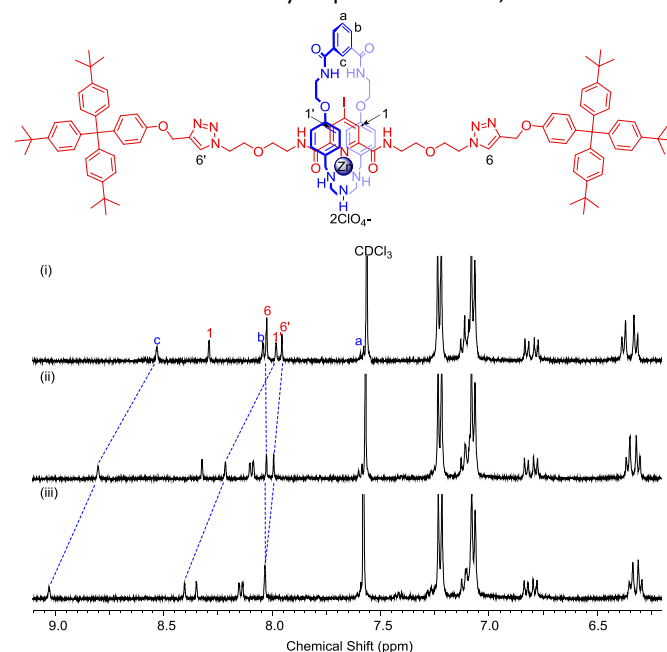


Figure 11. Partial ^1H NMR spectra of the [2]rotaxane **14**- $\text{Zn}(\text{ClO}_4)_2$ in the presence of (i) 0, (ii) 1 and (iii) 5 equivalents of TBACl in $\text{CDCl}_3:\text{CD}_3\text{OD}:\text{D}_2\text{O}$ 45:45:10 at 298 K.

nitrate anions. The iodo-functionalised [2]rotaxane **14**- $\text{Zn}(\text{ClO}_4)_2$ displays broadly comparable but slightly higher anion binding affinities than the C—H hydrogen bonding control system **15**- $\text{Zn}(\text{ClO}_4)_2$. In particular nitrate and iodide are bound with noticeably higher affinities by the rotaxane bearing an iodine substituent. The differing anion recognition behaviours displayed by rotaxane hosts **14**- $\text{Zn}(\text{ClO}_4)_2$ and **15**- $\text{Zn}(\text{ClO}_4)_2$ are best explained by an interplay between size complementary considerations and subtle differences in host solvation and pyridyl C—H bond polarisation ensuing from the presence of the lipophilic and electronegative iodine substituent, along with a possible contribution from C—I \cdots X[−] halogen bonding interactions for the iodo-functionalised [2]rotaxane **14**- $\text{Zn}(\text{ClO}_4)_2$. In general the presence of the iodine substituent results in only modest improvements in the receptor's anion recognition capabilities, suggesting that the

C—I·····X[−] XB contribution to anion binding by the [2]rotaxane **14**·Zn(ClO₄)₂ is relatively minor, with Coulombic and C—H·····X[−] and N—H·····X[−] HB interactions playing a more dominant role, or that the steric requirements of the iodine atom do not allow for favourable XB and HB interactions between the rotaxane's macrocycle component isophthalamide and axle component iodopyridyl groups to occur in a fully synergistic manner.

Conclusions

Three new heteroditopic [2]rotaxane ion-pair host systems which contain axle separated interlocked binding cavities for an anion and a transition metal cation were synthesised using a copper(II) directed passive metal template strategy. ¹H NMR titration experiments revealed the [2]rotaxanes are capable of cooperatively binding halide and nitrate anions in the presence of a co-bound zinc(II) cation. The hydrogen-bonding [2]rotaxane **8**·Zn(ClO₄)₂ was found to bind chloride and bromide selectively over nitrate and iodide anions in a competitive protic CDCl₃:CD₃OD 1:1 solvent mixture. The related [2]rotaxane host system **14**·Zn(ClO₄)₂ which contains a potential iodopyridine XB donor group, and a C—H HB control system **15**·Zn(ClO₄)₂ were both found to display enhanced affinities for bromide and iodide with respect to chloride in a more competitive CDCl₃:CD₃OD:D₂O 45:45:10 aqueous-organic solvent mixture. Subtle differences between the anion recognition properties of the XB functionalised rotaxane **14**·Zn(ClO₄)₂ and HB analogue **15**·Zn(ClO₄)₂ were observed, suggesting that the XB contribution to anion binding by the [2]rotaxane **14**·Zn(ClO₄)₂ is relatively minor, with Coulombic and C—H·····X[−] and N—H·····X[−] HB interactions playing a more dominant role.

Conflicts of interest

There are no conflicts to declare.

Acknowledgements

We thank the European Research Council (under the European Union's 7th Framework programme (FP7/2007–2013), ERC advanced grant agreement number 267426) and the University of Oxford for funding. We also thank Dr Kirsten Christensen and Dr Amber Thompson for their generous help and advice with crystallographic data collection and refinement, Diamond Lightsource for an award of beamtime on I19 (MT13639) and the beamline scientists (Drs David Allan, Mark Warren, Harriott Nowell, and Sarah Barnett) for technical support.

Notes and references

- † Crystallographic data (including structure factors) have been deposited with the Cambridge Crystallographic Data Centre (CCDC 1560763–1560766). Full refinement details are provided in the ESI.
- § When the titration experiments were attempted in CDCl₃:CD₃OD 1:1 the equilibria appeared to be more complex and we were unable to obtain quantitative binding

data. As well as observing gradual shifts in the ¹H NMR signals, an extra set of peaks was observed to appear in slow exchange with the original signals, possibly indicating a competing binding mode involving direct binding of the anion to the metal cation in a contact ion-pair fashion.

- φ The non-interlocked axle components of the [2]rotaxanes **8** and **14** were isolated as side-products of the rotaxane synthesis reactions.

- 1 J. L. Sessler, P. A. Gale and W.-S. Cho, *Anion Receptor Chemistry*, Royal Society of Chemistry, 2006.
- 2 N. H. Evans and P. D. Beer, *Angew. Chem. Int. Ed.*, 2014, **53**, 11716–11754.
- 3 N. Busschaert, C. Caltagirone, W. Van Rossom and P. A. Gale, *Chem. Rev.*, 2015, **115**, 8038–8155.
- 4 A. Caballero, F. Zapata and P. D. Beer, *Coord. Chem. Rev.*, 2013, **257**, 2434–2455.
- 5 S. K. Kim and J. L. Sessler, *Chem. Soc. Rev.*, 2010, **39**, 3784–3809.
- 6 A. J. McConnell and P. D. Beer, *Angew. Chem. Int. Ed.*, 2012, **51**, 5052–5061.
- 7 M. J. Deetz, R. Shukla and B. D. Smith, *Tetrahedron*, 2002, **58**, 799–805.
- 8 M. J. Barrell, D. A. Leigh, P. J. Lusby and A. M. Z. Slawin, *Angew. Chem. Int. Ed.*, 2008, **47**, 8036–8039.
- 9 C. Allain, P. D. Beer, S. Faulkner, M. W. Jones, A. M. Kenwright, N. L. Kilah, R. C. Knighton, T. J. Sørensen and M. Tropiano, *Chem Sci*, 2013, **4**, 489–493.
- 10 M. J. Langton, O. A. Blackburn, T. Lang, S. Faulkner and P. D. Beer, *Angew. Chem. Int. Ed.*, 2014, **53**, 11463–11466.
- 11 R. C. Knighton and P. D. Beer, *Chem. Commun.*, 2014, **50**, 1540–1542.
- 12 N. H. Evans, C. J. Serpell and P. D. Beer, *Chem. Commun.*, 2011, **47**, 8775–8777.
- 13 L. M. Hancock, E. Marchi, P. Ceroni and P. D. Beer, *Chem. – Eur. J.*, 2012, **18**, 11277–11283.
- 14 J. Lehr, T. Lang, O. A. Blackburn, T. A. Barendt, S. Faulkner, J. J. Davis and P. D. Beer, *Chem. – Eur. J.*, 2013, **19**, 15898–15906.
- 15 J. Y. C. Lim, M. J. Cunningham, J. J. Davis and P. D. Beer, *Dalton Trans.*, 2014, **43**, 17274–17282.
- 16 A. Brown, M. J. Langton, N. L. Kilah, A. L. Thompson and P. D. Beer, *Chem. – Eur. J.*, 2015, **21**, 17664–17675.
- 17 M. J. Langton, I. Marques, S. W. Robinson, V. Félix and P. D. Beer, *Chem. – Eur. J.*, 2016, **22**, 185–192.
- 18 In a related example, an ion-pair rotaxane host system which binds anions in the presence of a co-bound tetrabutylammonium cation has recently been reported: J. R. Romero, G. Aragay and P. Ballester, *Chem. Sci.*, 2016, **8**, 491–498.
- 19 S. Saha, I. Ravikumar and P. Ghosh, *Chem. Commun.*, 2011, **47**, 6272–6274.
- 20 L. C. Gilday and P. D. Beer, *Chem. – Eur. J.*, 2014, **20**, 8379–8385.
- 21 C. J. Massena, A. M. S. Riel, G. F. Neuhaus, D. A. Decato and O. B. Berryman, *Chem Commun*, 2015, **51**, 1417–1420.
- 22 V. Amendola, G. Bergamaschi, M. Boiocchi, N. Fusco, M. V. L. Rocca, L. Linati, E. L. Presti, M. Mella, P. Metrangolo and A. Miljkovic, *RSC Adv.*, 2016, **6**, 67540–67549.
- 23 A. Brown and P. D. Beer, *Chem. Commun.*, 2016, **52**, 8645–8658.
- 24 S. Saha, B. Akhuli, S. Chakraborty and P. Ghosh, *J. Org. Chem.*, 2013, **78**, 8759–8765.
- 25 S. Santra, S. Mukherjee, S. Bej, S. Saha and P. Ghosh, *Dalton Trans.*, 2015, **44**, 15198–15211.
- 26 A. W. Addison, T. N. Rao, J. Reedijk, J. van Rijn and G. C. Verschoor, *J. Chem. Soc., Dalton Trans.*, 1984, 1349–1356.
- 27 S. Saha, I. Ravikumar and P. Ghosh, *Chem. – Eur. J.*, 2011, **17**, 13712–13719.

- 28 S. Saha, S. Santra and P. Ghosh, *Eur. J. Inorg. Chem.*, 2014, **2014**, 2029–2037.
- 29 S. Saha, S. Santra, B. Akhuli and P. Ghosh, *J. Org. Chem.*, 2014, **79**, 11170–11178.
- 30 F. D. Barb, O. Netoiu, M. Sorescu and M. Weiss, *Comput. Phys. Commun.*, 1992, **69**, 182–186.
- 31 H. Zheng, W. Zhou, J. Lv, X. Yin, Y. Li, H. Liu and Y. Li, *Chem. - Eur. J.*, 2009, **15**, 13253–13262.
- 32 V. Aucagne, K. D. Hänni, D. A. Leigh, P. J. Lusby and D. B. Walker, *J. Am. Chem. Soc.*, 2006, **128**, 2186–2187.
- 33 M. J. Hynes, *J. Chem. Soc., Dalton Trans.*, 1993, 311–312.
- 34 D. Curiel and P. D. Beer, *Chem. Commun.*, 2005, 1909–1911.